Overall rectification and second harmonic generation of space charge waves

M. P. Petrov and V. V. Bryksin
Physico-Technical Institute, Russian Academy of Sciences, St. Petersburg 194021, Russia

H. Vogt, F. Rahe, and E. Krätzig
University of Osnabrück, Physics Department, D-49080 Osnabrück, Germany
(Received 27 March 2002; published 6 August 2002)

The effects of overall rectification and second-harmonic generation of space-charge waves in photorefractive crystals were reliably detected. The effect of overall rectification results in variations of the dc current flowing in a circuit containing a photorefractive crystal and a voltage source when space-charge waves are excited in the crystal. In the experiments, variations in the dc current reached 20%. Two mechanisms responsible for second-harmonic generation were experimentally revealed. The theory of the observed effects is briefly described.

DOI: 10.1103/PhysRevB.66.085107 PACS number(s): 42.40.Eq, 42.70.Nq, 73.20.Mf, 42.65.Hw

I. INTRODUCTION

Space-charge waves (SCW) are eigenmodes of oscillation in a system of traps and free carriers in semi-insulating solids[1] when carriers move in an electric field. Initially,[1] these waves were termed trap recharging waves, which means that their nature is associated with trap charging and discharging by free carriers excited thermally or by illuminating the sample, and their propagation is due to the influence of an applied electric field. Sometimes SCW are referred to as ''spastrons,''[2] because they are regarded as new quasiparticles in solids, or ''photorefractons'' if they are studied in photorefractive crystals.[3] However, more often the term ''space-charge waves'' is used. SCW exhibit very specific properties;[1] for instance, their wave vector is inversely proportional to their frequency, so phase and group velocities are oppositely directed. The propagation direction of these waves is determined by the direction of the electric field applied to the crystal; they do not exhibit time inversion symmetry. The free path length of SCW is typically limited by the carrier drift length, and these waves are strongly attenuated.

SCW are of great interest for photorefractive crystals[4] (in particular, for the sillenite family $Bi_{12}MO_{20}$, where $M=$ Si, Ti, or Ge) because dynamic properties of the crystals in the presence of an external electric field (processes of holographic recording, hologram relaxation, oscillations of holographic gratings) are very often determined by these waves. SCW can play an important role in semi-insulating semiconductors, for instance, GaAs,[5] InP:Fe, CdTe:V,[6,7] and other materials. The SCW excitation can provide a considerable increase in the sensitivity of devices based on the principles of dynamic holography.[8] It can be supposed that some transient phenomena in photoreceivers and other semiconductor devices[9,10] are associated with SCW as well.

Experimentally, SCW were detected for the first time in *n*-type Ge:Au by measuring the impedance as a function of applied voltage.[11] However, the electrical technique of SCW excitation encounters serious experimental difficulties in the selective excitation of SCW with a desired set of parameters. A much more flexible and informative technique of SCW investigation includes optical excitation of SCW by illuminating the crystal with a periodical interference pattern (a recording interference pattern). For instance, in Refs. 12,13 the crystal was illuminated by a moving interference pattern with a grating spacing equal to the period of the corresponding space-charge wave and with a velocity equal to that of the space-charge wave. Then the pulse detection technique[14,15] and the technique of detection of parametric excitation[16] were suggested. The theory of the parametric effect was developed (see, for instance, Ref. 17). Selection of the experimental method for investigations of SCW is of great importance because the obtained information depends very much on the technique used for SCW excitation and detection. In this work we used the technique of optical excitation of SCW by an oscillating interference pattern.[3] To detect nonlinear effects, we used both optical and electrical techniques.

If SCW are optically excited, two main regimes can be considered. The first one is the linear regime when only effects proportional to the first power of the contrast ratio m of the interference pattern are taken into account. The second one is the nonlinear regime, in which effects proportional to m^2 (or a higher power of m) become important. For the effects proportional to m^2 the situation formally reminds of the second-order nonlinearity in optics,[18] and one can expect that phenomena similar to second-order nonlinear effects in optics (second-harmonic generation, rectification[19]) exist in the system of SCW. Moreover, as will be shown below, the employed technique of optical excitation of SCW by illuminating the sample by an oscillating interference pattern results in the simultaneous excitation of SCW and formation of a static space-charge grating, whose spacing is equal to the spatial period of SCW. In this case new nonlinear effects unknown in nonlinear optics can be found. They are spatial doubling (when doubling of the SCW wave vector occurs without frequency doubling) and spatial rectification (when a spatially homogeneous electric field oscillating with the frequency of the SCW arises). Note that the electric-field waves resulting from second-harmonic generation (overall doubling) or spatial doubling can be both, eigenmodes and forced modes of the system under consideration, but nevertheless both types of modes can easily be detected.

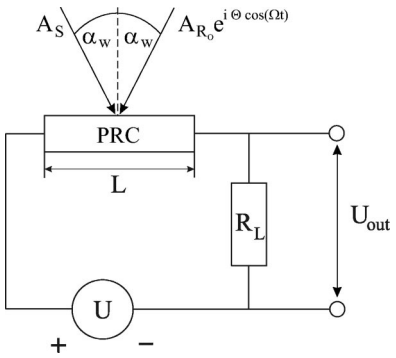

FIG. 1. Diagram demonstrating our method of SCW excitation and detection of overall rectification: PRC is the photorefractive crystal, U is the applied voltage, R_L is the loading resistor, U_{out} is the voltage across loading resistor, and α_W is the writing angle.

In this paper, we present in detail the experimental investigation of overall rectification and second-harmonic generation (overall doubling) of space-charge waves and briefly describe the developed theory of these effects. We also briefly discuss the effects of partial (spatial) doubling and partial (spatial) rectification. Some very preliminary data were published in Ref. 20.

In the experiments described in the present paper, we used the technique of excitation of SCW by an oscillating interference pattern formed by two laser beams, one of which was phase-modulated. The nonlinear effects were detected by using either light diffraction from the refractive index grating caused by the electric fields of SCW (second-harmonic generation) or measurements of the dc voltage across the loading resistance (overall rectification).

II. THEORETICAL BACKGROUND

Here we briefly describe the theory of overall rectification and second-harmonic generation for SCW in photorefractive crystals. The detailed theory will be published elsewhere.

A. Linear approach

We consider a photorefractive crystal placed into an external electric field and illuminated by an oscillating interference pattern formed by two beams, one of which is phase modulated (Fig. 1). The interference pattern is given by

$$W(x,t)=W_0[1+m\cos(K_g x+\Theta\cos\Omega t)] \tag{1}$$

with

$$W_0=(W_S+W_R). \tag{2}$$

Here W_S and W_R are the intensities of the recording beams, $\Omega=2\pi f$, where f is the phase modulation frequency, Θ is the phase modulation amplitude, m is the contrast ratio of the interference pattern, $K_g=2\pi/\Lambda$, and Λ is the interference pattern spacing. For a symmetrical recording scheme, we obtain

$$\Lambda=\frac{\lambda_W}{2\sin\alpha_W}, \tag{3}$$

where λ_W is the recording light wavelength and α_W is the angle of incidence of the recording beams. Under illumination, photogeneration $g(x,t)$ of carries with the generation rate

$$g(x,t)=g_0[1+m\cos(K_g x+\Theta\cos\Omega t)] \tag{4}$$

occurs. Here, $g_0=HW_0$, and H is a coefficient determined by the photon energy, quantum efficiency of the process, and light absorption by the crystal. The photoexcited carriers (in our case electrons) drift from illuminated regions under the action of the applied field and are captured by traps. The distribution of photoexcited carriers can be presented as a sum of a static grating and, for the approximation $\Theta\ll 1$, two gratings moving in opposite directions,

$$\begin{aligned} g(x,t)&=g_0 t[1+m\cos(K_g x+\Theta\cos\Omega t)]\\ &\approx g_0+g_0 m\cos K_g x-\frac{1}{2}g_0 m\Theta\sin(K_g x+\Omega t)\\ &\quad-\frac{1}{2}g_0 m\Theta\sin(K_g x-\Omega t). \end{aligned} \tag{5}$$

In such a way, a nonuniform (static and dynamic) charge distribution is formed in the photorefractive crystal. When K_g and Ω of the excited gratings coincide with the wave vector and frequency of the space-charge wave, respectively, a resonance excitation of SCW occurs.

To calculate the internal field $E(x,t)$ caused by the space-charge distribution, we use the conventional system of equations[21,22]

$$\frac{n(x,t)}{\tau}-\frac{1}{e}\frac{\partial j(x,t)}{\partial x}=g(x,t), \tag{6}$$

$$j(x,t)=e\mu n(x,t)[E_0+E(x,t)], \tag{7}$$

$$\frac{\epsilon}{4\pi}\frac{\partial E(x,t)}{\partial t}+j(x,t)=I(t). \tag{8}$$

Here $j(x,t)$ is the nonhomogeneous ohmic current density, $n(x,t)$ is the density of photoexcited carriers, τ is the carrier lifetime in the conduction band, μ is the carrier mobility, ϵ is the static permittivity, E_0 is the electric field determined as U/L, where U is the applied voltage, L is the distance between the electrodes, and $I(t)$ is the current density in the outside circuit defined as the full current in the outside circuit divided by the cross sectional area S of the crystal. In Eq. (7), the contribution from the diffusion process is omitted, since it is assumed that at high E_0 and relatively small K_g the diffusion processes can be neglected.

Usually the complementary condition

$$\int_0^L E(x,t)\,dx=0 \tag{9}$$

is used[21] to solve the Eqs. (6)–(8). Relationship (9) means that the induced space-charge grating does not form a homogeneous electric field in the crystal. This is quite correct if there are no resistors (a real loading resistor R_L, or an internal resistance of the voltage source, or a resistance of nonohmic contacts) connected in series with the crystal. In our consideration, all these contributions are taken into account by including into consideration an effective loading resistor R. Then instead of Eq. (9), we use the expression[23]

$$\frac{1}{L}\int_0^L dx E(x,t) = -I(t)\rho, \tag{10}$$

where $\rho = RS/L$.

Actually, according to condition (10), the applied field inside the crystal becomes lower than E_0 due to a voltage drop at the resistor R. The use of condition (10) implies that space-charge gratings can give rise, in certain situations, to a static or alternating electric field (homogeneous along the crystal length).

At the next step of the calculation, the density $n(x,t)$ is excluded from the equations Eqs. (6)–(8) and the temporal and spatial Fourier components of the space-charge field and current density are determined. As a result, in the linear approximation ($m \ll 1$ and $\Theta \ll 1$), the first (spatial and temporal) Fourier component $Y_{1,1}$ of the space-charge field (in relative units) is

$$Y_{1,1} = \frac{m}{4i(1+q)} \frac{\Theta}{1+\omega\tilde{d}+i\omega}, \tag{11}$$

and the magnitudes of $Y_{p,l}$ for $l,p=-1$ can be obtained from following relationship:

$$Y_{-p,-l} = Y_{p,l}^*, \quad Y_{p,-l}(\omega) = Y_{p,l}(-\omega). \tag{12}$$

Here p and l denote spatial and temporal Fourier components, respectively, $q = \rho\sigma, \sigma = \epsilon/(4\pi\tau_M) = e\mu g_0 \tau$ is the conductivity under uniform illumination (the dark conductivity is neglected), τ_M is the Maxwell relaxation time, $\omega = \Omega\tau_M, \tilde{d} = d/(1+q), d = K_g L_0$, and $L_0 = \mu\tau E_0$ is the carrier drift length. Note that the parameter d (parameter of quality) and the drift length are introduced for the case when the applied field equals E_0. If the resistance R is taken into account and, hence, the internal field differs from E_0, the drift length and the parameter d are reduced by a factor $(1+q)$; that is why the parameter $\tilde{d}$ appears.

In accordance with Eqs. (11) and (12), the space-charge field of the SCW having a wave vector K_g and oscillating with the frequency $f = \Omega/2\pi$ is determined as

$$E_{SC}(x,t)_{1,1} = E_0[Y_{1,1}(\omega)\exp(i\Omega t) + Y_{1,-1}(\omega)\exp(-i\Omega t)]\exp(iK_g x). \tag{13}$$

As one can see from Eqs. (11) and (12) (when $l=-1$), there is a resonance when the condition $\omega\tilde{d}=1$ is fulfilled. This means that resonance excitation of SCW takes place. The resonance frequency f_f (or fundamental frequency) for $\tilde{d} \gg 1$ is

$$f_f = \frac{\Omega_f}{2\pi} = \frac{1}{2\pi\tau_M\tilde{d}} = \frac{1+q}{2\pi\tau_M\mu\tau E_0 K_g}. \tag{14}$$

For the approximation used here, expression (14) is the dispersion law for the SCW. At resonance, the real magnitude of the SCW electric field is

$$\mathrm{Re}\, E_{SC}(x,t)_{1,1} = \frac{m\Theta d E_0}{4(1+q)^2}\cos(\Omega t - K_g x). \tag{15}$$

The expression for the frequency dependence of $\mathrm{Re}\, E_{SC}(x,t)_{1,1}$ can be found in. Ref. 3

B. Overall rectification

Let us discuss the origin of the nonlinear effects. Expression (7) for the current density includes the product $n(x,t)E(x,t)$. The space-charge field of SCW, as follows from Eq. (15), is proportional to $m\Theta[\exp i(\Omega t - K_g x) + \text{c.c.}]$. In addition, it can be shown that the charge density $n(x,t)$ is also proportional to $m\Theta[\exp i(\Omega t - K_g x) + \text{c.c.}]$. So, in Eq. (7) terms proportional to $m^2\Theta^2[\exp i(2\Omega t - 2K_g x) + \text{c.c.}]$ and $m^2\Theta^2 \times \text{const.}$ arise. The first term means doubling of the wave vector and the frequency of the SCW, i.e., second-harmonic generation, while the second term describes overall (spatial and temporal) rectification of SCW. The latter effect is formally analogous to rectification of light waves due to a second-order nonlinearity.[19] The difference is that, in optics, rectification gives rise to a homogeneous and constant polarization, whereas in the system of SCW it causes an additional homogeneous, permanent component of the current. Since detailed calculations will be published elsewhere, below we present the final expression for the dc current density I_0 taking into account the effect of rectification. At $\Theta \ll 1$, the relationship has a rather simple form

$$I_0(\omega) = \frac{\sigma E_0}{1+q}\left\{1 - \frac{m^2}{2(1+q)} + \frac{m^2\Theta^2}{8(1+q)} \times \left[2 - \frac{1}{(1-\omega\tilde{d})^2+\omega^2} - \frac{1}{(1+\omega\tilde{d})^2+\omega^2}\right]\right\}. \tag{16}$$

Actually this expression describes the situation quite well up to $\Theta = 1$. As one can see from Eq. (16), the dc current in the outside circuit depends on the phase modulation frequency of the recording beam and has a minimum near the frequency of resonance excitation of SCW $\omega = 1/\tilde{d}$, or, to be more exact, the minimum occurs at $\omega_R^2 = [2\tilde{d} - (\tilde{d}^2+1)^{1/2}]/(\tilde{d}^2+1)^{3/2}$. Comparison of the theoretical expres-

sion with the experimental dependence I_0 formally allows one to find the magnitudes of $q, \tilde{d}$, and τ_M.

For arbitary value of Θ, the expression for I_0 has a more complicated form

$$I_0(\omega) = \frac{\sigma E_0}{1+q}\left\{1 - \frac{m^2}{2(1+q)}\sum_{l=-\infty}^{\infty}\frac{J_l^2(\Theta)}{(1-\omega\tilde{d}l)^2+\omega^2 l^2}\right\}$$

$$= \frac{\sigma E_0}{1+q}\left\{1 - \frac{m^2}{(1+q)\omega}\mathrm{Re}\int_0^{\infty} d\phi \times \exp\left(-\frac{2\phi}{\omega - i\omega\tilde{d}}\right) J_0(2\Theta\sin\phi)\right\}. \quad (17)$$

Here $J_l[f(\Theta)]$ is the lth order Bessel function. Relationship (17) shows that for $\tilde{d} > 1$ the dependence of the dc current on the modulation frequency can have a set of minima with characteristic frequencies $\omega = 1/(\tilde{d}l)$. At small Θ, the deepness of the minimum decreases as Θ^{2l}, but at high Θ the deepness of the minima can grow with l.

C. Second-harmonic generation (overall doubling)

To analyze the processes of second-harmonic generation, we have to find the second (spatial and temporal) Fourier components $Y_{2,2}$ of the space-charge field. The corresponding calculations lead to

$$Y_{2,2} = -\frac{m^2\Theta^2}{16(1+q)}\frac{1+i\omega}{1+4\omega\tilde{d}+2i\omega} \times \left[\frac{1}{1+2\omega\tilde{d}+2i\omega} + \frac{1}{(1+\omega\tilde{d}+i\omega)^2}\right] \quad (18)$$

and

$$Y_{2,-2}(\omega) = Y_{2,2}(-\omega). \quad (19)$$

Here the Fourier components are represented in relative units. Then the electric field of the space-charge wave having the wave vector $2K_g$ and oscillating with the frequency $2f$ (though the phase modulation occurs at f) is

$$E_{SC}(x,t)_{2,2} = E_0[Y_{2,2}(\omega)\exp(i2\Omega t) + Y_{2,-2}(\omega)\exp(-i2\Omega t)]\exp(i2K_g x). \quad (20)$$

It is seen from Eqs. (18) and (19) that the amplitude of the space-charge wave having a doubled wave vector and a doubled temporal frequency has three resonance maxima. The first one corresponds to $\omega = 1/\tilde{d}$, the second one corresponds to $\omega = 1/2\tilde{d}$, and the third one corresponds to $\omega = 1/4\tilde{d}$. The physical origins of these three resonances are quite clear.

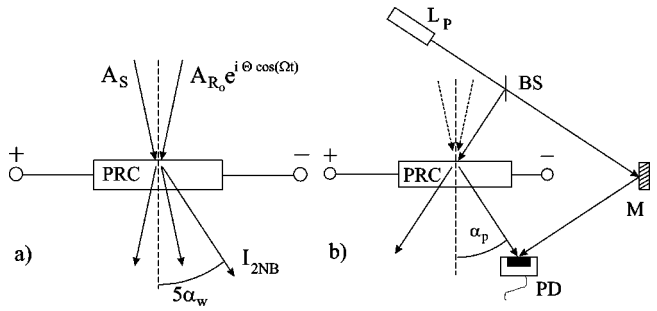

FIG. 2. Diagram demonstrating the detection of the second harmonic of SCW by measuring (a) the second-order-non-Bragg diffraction of one of the recording beams, (b) the diffraction of the probe beam from the grating with $2K_g$ recorded with the beams A_S and A_R showed by the dashed arrows. PRC is the photorefractive crystal, L_P is the laser radiating the probe beam, BS is the beam splitter, M is the the mirror, and PD is the photodetector.

The resonance at $\omega = 1/4\tilde{d}$ originates from the interaction of two forced waves having the wave vectors K_g and the dimensionless frequencies $\omega = 1/4\tilde{d}$. The interaction of these waves results in a new wave with the wave vector $2K_g$ and the frequency $\omega = 1/2\tilde{d}$. This combination of magnitudes of the wave vector and frequency obeys the dispersion law for SCW, that means that the new wave resulting from the interaction of two forced waves is an eigenmode of the system and exhibits resonance excitation. On the contrary, the resonance at $\omega = 1/\tilde{d}$ corresponds to the resonance excitation of two eigenmodes that creates finally a forced wave with the wave vector $2K_g$ and the frequency $\omega = 1/2\tilde{d}$ via spatial and temporal doubling. Both these effects are proportional to the second power of the contrast ratio m and the phase modulation amplitude Θ. The third resonance (at $\omega = 1/2\tilde{d}$) has nothing in common with second-harmonic generation. It is associated with the fact that expansion of Eq. (5) contains terms proportional to Θ^2 (omitted before) and, hence, this fact should be taken into account when we consider the effects of second order with respect to Θ. These terms contain oscillations of the interference pattern at $2f$ (in spite of the fact that the phase modulation is at f), and when $\omega = 1/2\tilde{d}$, i.e., $\Omega = 1/(2\tau_M\tilde{d})$, resonance excitation of SCW with $2K_g$ occurs.

To detect second-harmonic generation, one can use diffraction experiments. One of the ways is to detect the second non-Bragg diffraction peak [Fig. 2(a)] and use a lock-in amplifier at the doubled frequency (excitation at f, but detection at $2f$). In this experiment, diffraction from the refractive index grating formed by $E_{SC}(x,t)_{2,2}$ (i.e., from the grating with the wave vector $2K_g$) through the Pockels electro-optic effect is detected. In this case the complex amplitude ($\delta J_{2,2}$) of the light intensity of the detected output signal is

$$\delta J_{2,2}(\omega)=\frac{1}{64}G^2A_{R0}^2m^4\Theta^2\frac{E_0^2}{(1+q)^2}\left\{\frac{(2+i\omega)^2}{[(1+i\omega)^2-\omega^2\tilde{d}^2][(1+i\omega)^2-4\omega^2\tilde{d}^2]}-\frac{1+i\omega}{1+4\omega\tilde{d}+2i\omega}\right.$$
$$\left.\times\left[\frac{1}{1+2\omega\tilde{d}+2i\omega}+\frac{1}{(1+\omega\tilde{d}+i\omega)^2}\right]-\frac{1+i\omega}{1-4\omega\tilde{d}+2i\omega}\left[\frac{1}{1-2\omega\tilde{d}+2i\omega}+\frac{1}{(1-\omega\tilde{d}+i\omega)^2}\right]\right\}. \quad (21)$$

Here G is a parameter that includes the effective electro-optic coefficient of the crystal depending on the crystal orientation and on the incident light polarization. In calculating Eq. (21), all components diffracted in the direction of the second non-Bragg diffraction peak (including diffraction from the static grating) were taken into account. In the general case, the expression for the observable value of the output signal $J_{2,2}$ is too complicated. Below we present the expression for the case when $\tilde{d}\gg 1$ and attenuation is ignored. Then we find

$$J_{2,2}(t)=\frac{1}{16}G^2A_{R0}^2m^4\Theta^2\frac{E_0^2}{(1+q)^2}\cos(2\Omega t)$$
$$\times\left\{\frac{2}{(1-\omega^2\tilde{d}^2)(1-4\omega^2\tilde{d}^2)}\right.$$
$$-\frac{(1+8\omega^2\tilde{d}^2)}{(1-4\omega^2\tilde{d}^2)(1-16\omega^2\tilde{d}^2)}$$
$$\left.-\frac{(1+9\omega^2\tilde{d}^2)}{(1-\omega^2\tilde{d}^2)^2(1-16\omega^2\tilde{d}^2)}\right\}. \quad (22)$$

Here we omitted the signal phase shift (which also depends on ω).

Note that the terms of Eqs. (21) and (22) describing the resonance at $\omega=1/\tilde{d}$ are modified by a contribution of a ''parasitic'' signal. The nature of this contribution is associated with doubling of the signal frequency by the photodetector. As detailed analysis shows, the detected diffracted peak of the optical field is a sum of various contributions containing also a signal at f. However, the output signal is proportional to the light intensity, so the intensity contains an additional component oscillating at $2f$. To eliminate this contribution, the experimental setup can be modified to avoid frequency doubling by the photodetector. This can be achieved if the detection technique including a probe beam from another laser is used [Fig. 2(b)]. In this case the probe beam is incident on the crystal simultaneously with the recording beams. If the crystal is thick enough, the angle of incidence of the probe beam is selected to satisfy the Bragg condition for diffraction of the probe beam from the grating with the wave vector $2K_g$. The angle of incidence can be found from the condition

$$\sin\alpha_p=2\frac{\lambda_p}{\lambda_W}\sin\alpha_W. \quad (23)$$

Here λ_p is the wavelength of the probe beam. In the case of a thin crystal (thickness D satisfies the relationship $D\ll\Lambda^2 n_0/4\lambda_p$, where n_0 is the refractive index of the crystal), there are no specific requirements to α_p. Simultaneously with the diffracted beam, a reference beam from the same laser has to be directed on the photodetector. The intensity of the reference beam must be much higher than the diffracted beam intensity. To avoid formation of the interference pattern, both beams must be focused on the photodetector. The output signal has to be detected at $2f$, whereas the excitation frequency has to be f. Then the frequency dependence of the output signal amplitude of interest will be

$$J_{2,2}(\omega)=\frac{GE_0m^2\Theta^2|A_RA_p|}{16(1+q)[(1-\omega\tilde{d})^2+\omega^2]}$$
$$\times\sqrt{\frac{(1+\omega^2)[(2-4\omega\tilde{d}+\omega^2\tilde{d}^2-\omega^2)^2+4\omega^2]}{[(1-4\omega\tilde{d})^2+4\omega^2][(1-2\omega\tilde{d})^2+4\omega^2]}}. \quad (24)$$

Here, A_R and A_p are the reference and probe beam amplitudes, respectively. For the sake of simplicity some terms that do not affect resonance characteristics of the output signal were ignored in calculating Eq. (24). As mentioned above, the technique involving the probe and reference beams allows one to detect both resonance peaks associated with the second-harmonic generation of SCW without distortions. If no reference beam is used, the output signal is described by Eq. (22), where the recording beam intensity must be replaced by the probe beam intensity. However, in this case, as mentioned above, the second resonance is distorted by the additional signal resulting from frequency doubling by the photodetector.

It can be found from Eq. (21) that the ratio between the observable signal intensities for different maxima as a function of $\tilde{d}$ is $J_{2,2}(f=f_f/4):J_{2,2}(f=f_f/2):J_{2,2}(f=f_f)\approx(68\tilde{d}/3):(19\tilde{d}):(\tilde{d}^2)$ and the similar ratio as a function of applied voltage is $J_{2,2}(f=f_f/4):J_{2,2}(f=f_f/2):J_{2,2}(f=f_f)\approx(68U^2/3):(19U^2):(U^3)$.

III. EXPERIMENTAL RESULTS

The experiments were performed with single crystals of $Bi_{12}GeO_{20}$ and $Bi_{12}SiO_{20}$. The most results were obtained for $Bi_{12}GeO_{20}$. The sample of $Bi_{12}GeO_{20}$ has the standard holographic [110] cut and was $(2.0\times4.0\times2.5)$ mm^3 in size, the light propagation was along the [110] axis, the grating wave vector and the applied field were directed along the

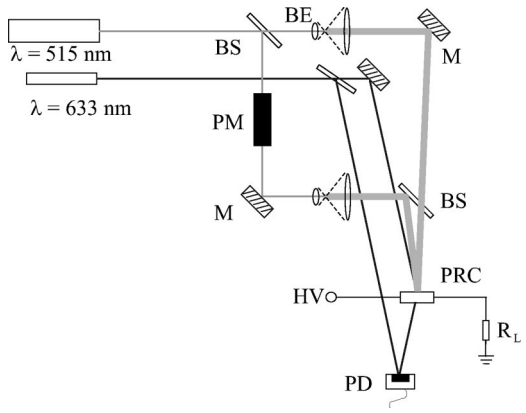

FIG. 3. Experimental setup (schematically); PRC is the photorefractive crystal, R_L is the loading resistor, HV is the high-voltage source, PM is the phase modulator, BE is the beam expander, BS is the beam splitter, *M* is the mirror, and PD is the photodetector.

[001] axis, and the crystal thickness was 2.0 mm. The sample of $Bi_{12}SiO_{20}$ has the same cut and was $(2.3\times4.0\times2.8)$ mm^3 in size. For recording, an argon-ion laser with an output power of 750 mW and a wavelength of 514 nm was used. The experimental setup is shown in Fig. 3. In the experiments with the probe beam, a He-Ne laser was used. For the experiments with overall rectification, a loading resistor of 100 kOhm was installed in series with the crystal.

A. Overall rectification

To detect variations of the dc current in the outside circuit, the voltage drop across the loading resistor was measured by a digital voltmeter. Figure 4 shows the measured voltage in arbitrary units as a function of the phase modulation frequency f for different phase modulation amplitudes Θ. Figure 5 shows a comparison of theoretical and experimental data for $\Theta=0.2\pi$ and for $\Theta=0.9\pi$ with the fitting parameters $q=0.7$, $\tilde{d}=3.6$, and $\tau_M=3.4\times10^{-4}$ s. From these data it follows immediately that the product $\mu\tau$ is equal to 1.6×10^{-7} cm^2/V, which is consistent with values known from literature.[17] Theoretical data for small Θ were obtained by

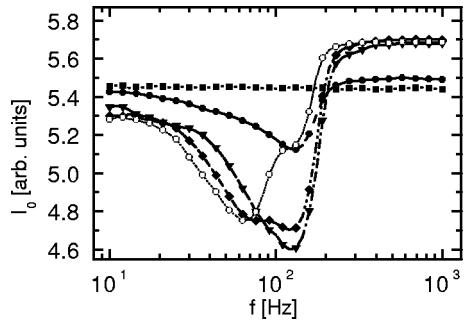

FIG. 4. dc current I_0 (in arbitrary units) as a function of the phase modulation frequency f for different amplitudes Θ of phase modulation: For $Bi_{12}GeO_{20}$ $E_0=8$ kV/cm, $\Lambda=13.1$ μm, $m=0.43$, and $W_0=130$ mW/cm^2; $-\blacksquare-$: $\Theta=0$, $-\bullet-$: $\Theta=0.2\pi$, $-\nabla-$: $\Theta=0.6\pi$, $-\blacklozenge-$: $\Theta=0.8\pi$, $-\circ-$: $\Theta=1.0\pi$. The lines are guides to the eye.

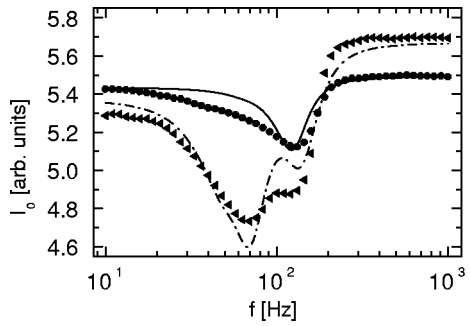

FIG. 5. Comparison between theory (lines) and experiment (symbols) for overall rectification in $Bi_{12}GeO_{20}$ (I_0 is the dc current, f is the phase modulation frequency): $\tilde{d}=3.6\pm0.5$, $\tau_M=3.4\times10^{-4}$ s, and $q=0.7$; $\Theta=0.2\pi$ (solid line, ●) and $\Theta=0.9\pi$ (dashed line, ◀).

using Eq. (16) and for $\Theta=0.9\pi$ by using Eq. (17). It can be seen from Fig. 5 that the theory agrees with the experiments quite well. At small Θ, there is one minimum at $f=f_f=130$ Hz, but at high Θ a second minimum at $f=f_f/2$ appears. As Θ increases, the second minimum becomes deeper than the first one. In Fig. 4 there is a very specific point at the frequency scale where all experimental curves for small Θ intersect. This fact is also in agreement with theoretical considerations because it follows from Eq. (16) that the expression in square brackets is zero at some specific frequency regardless of Θ. The magnitude of current at this point coincides within the experimental accuracy with the data corresponding to $\Theta=0$, which is also consistent with Eq. (16). The experimental dependence of the deepness of the minima on Θ at small Θ qualitatively obeys the law Θ^2 predicted by Eq. (16). Figure 6 shows the frequency position of the minimum as a function of applied field.

A very important parameter is the magnitude of the effect. The drop of the dc current at excitation of SCW reaches almost 20%. It is a giant effect. Figures 4–6 show the results obtained for $Bi_{12}GeO_{20}$. Figure 7 shows the detected voltage at the loading resistor as a function of phase modulation frequency for different grating spacings in $Bi_{12}SiO_{20}$, and Fig. 8 shows variations in the current corresponding to the current minimum versus grating spacing for the same crystal.

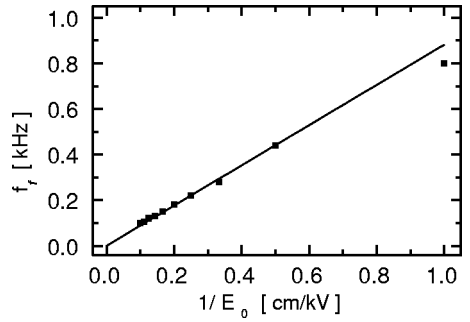

FIG. 6. Frequency position of the dc current minimum in $Bi_{12}GeO_{20}$ (resonance frequency f_f) as a function of applied field E_0: $\Lambda=13.1$ μm, $m=0.43$, $W_0=130$ mW/cm^2, and $\Theta=2$ rad. The solid line corresponds to a function $\propto 1/E_0$.

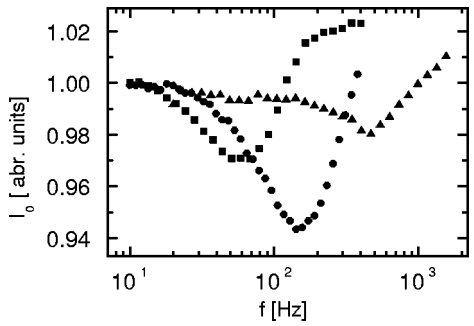

FIG. 7. dc current I_0 (in arbitrary units) as a function of the phase modulation frequency f for different grating spacings in $Bi_{12}SiO_{20}$ (▲: $\Lambda=50$ μm, ●: $\Lambda=12.6$ μm, ■: $\Lambda=5.5$ μm; $E_0=8$ kV/cm, $m=0.43$, $W_0=130$ mW/cm^2, and $\Theta=1$ rad).

B. Second-harmonic generation (overall doubling)

All experiments were performed with $Bi_{12}GeO_{20}$. In the experiments, a probe beam was used. Figures 9(a) and 9(b) show the diffraction intensity corresponding to diffraction of the probe beam from the grating with the wave vector $2K_g$ as a function of the modulation frequency for two gratings with different spacings. No reference beam was used here because of an insufficient stability of the setup. The use of a reference beam resulted in a too high phase noise. The data presented in Fig. 9 (in relative units) are the output signal intensities measured at $2f$ when the modulation frequency is f. As one can see from Fig. 9(a), the output signal exhibits three maxima as predicted by the theory. When the grating spacing decreases (the wave vector increases), the resonance frequencies are reduced in accordance with the dispersion law (14). In Fig. 9(b), only two resonances are clearly seen. This is because the intermediate resonance is not resolved at low frequencies. A gradual ''absorption'' of the intermediate resonance by the first resonance is clearly seen when the grating spacing is reduced step by step. Figure 10 shows the spectra of the output signal for three different values of applied field. The experimental dependences of the peak intensities on the applied field agree qualitatively with the predictions of the theory (21), however, the ratio between the intensities of the peaks does not correspond to the theory (the right peak is more intense than predicted by the theory) .

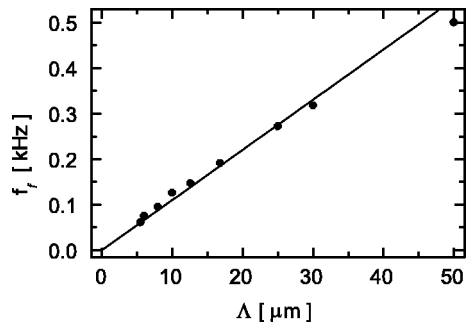

FIG. 8. Frequency position of the dc current minimum (resonance frequency f_f) in $Bi_{12}SiO_{20}$ as a function of grating spacing Λ ($E_0=8$ kV/cm, $m=0.43$, $W_0=130$ mW/cm^2, and $\Theta=1$ rad). The solid line corresponds to a function $\propto\Lambda$.

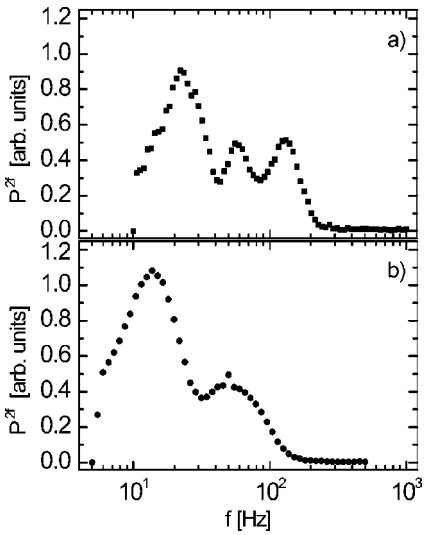

FIG. 9. Output signal P^{2f} at $2f$ as a function of modulation frequency f for two grating spacings in the experiments for the detection of second-harmonic generation in accordance with Fig. 2(b), with no reference beam. For $Bi_{12}GeO_{20}$ $E_0=8$ kV/cm, $m=0.43$, $W_0=130$ mW/cm^2, $\Theta=1$ rad; (a) $\Lambda=13$ μm; (b) $\Lambda=7$ μm.

IV. DISCUSSION

The obtained experimental results unambiguously demonstrate the existence of the effects of overall rectification and second-harmonic generation of SCW. A more detailed comparison of the theoretical model with experiments can be made for the effect of rectification because of the simplicity of the experiments and the theoretical expressions [for instance, Eq. (16)] describing the experimental data. The effect of overall rectification is not a specific effect for photorefractive crystals. This effect has a general character, for instance, it can be found in many semi-insulating semiconductors or, more generally speaking, in any nonlinear system with unidirectional propagation of charge carrier waves. The effect of rectification results in an additional dc component [$\delta I_0(\omega)$] of the current flowing through the crystal and reduction of the total dc current. The current of rectification does not cause any changes in the voltage on the crystal if there is no real or effective loading resistance in the circuit, since in the

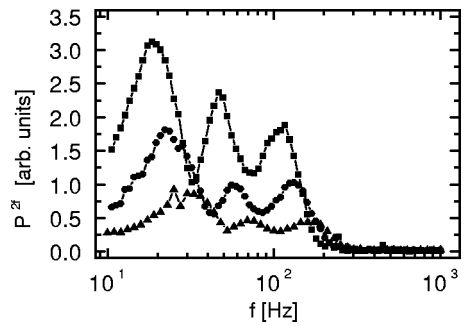

FIG. 10. Frequency dependence of the output signal P^{2f} at $2f$ for different applied fields E_0. For $Bi_{12}GeO_{20}$ $m=0.43$, $W_0=130$ mW/cm^2, $\Theta=1$ rad, $\Lambda=13$ μm; ■: $E_0=10$ kV/cm, ●: $E_0=8$ kV/cm, ▲: $E_0=6$ kV/cm. The lines are guides to the eye.

absence of a loading resistance the voltage affecting the crystal is determined by the source of voltage alone. However, it is interesting to estimate an equivalent voltage $U_{eq} = U\delta I_0(\omega)/I_0(0)$, which could cause the same variations in the current magnitude. Here, $I_0(0)$ is the dc current when there is no phase modulation of the recording beam. At resonance, U_{eq} reaches 1–2 kV, which is seven orders of magnitude higher than the value detected in nonlinear optics due to the effect of rectification.[19]

It can be stated that almost all predictions of the theory developed here agree with the experiments. The order of magnitude of the effect is consistent with the theoretical estimates. The expression for the frequency dependence describes the experimental data quite well. The positions of the resonance frequencies as functions of various parameters are in a good agreement with theoretical predictions. One minimum is detected at low Θ, and the other minimum at half the fundamental frequency arises at higher Θ in accordance with Eq. (17). The frequency position of the main minimum (at low Θ) changes in accordance with the dispersion law (14), when the grating spacing and applied field are varied (Figs. 6 and 8). Deviations from the theoretical straight lines at low values of E_0 and large values of Λ are associated with the aspect that formula (14) is only correct for $d \gg 1$, but this requirement is not satisfied at low E_0 and large Λ. The slope of the linear dependence f_f as a function of $1/E_0$ in Fig. 6 is in agreement with calculated values using the above-mentioned fitting parameters d, τ_M, q, and $\mu\tau$.

From the theoretical point of view the dispersion law (14) must be modified in the case of a strong nonlinearity of the system. It is a typical situation when the resonance frequency (as well as the attenuation) is renormalized in nonlinear oscillating systems. This renormalization can be found by detailed and rather tedious calculations. The expression for the resonance frequency f_f becomes

$$f_f \approx \frac{1}{2\pi\tau_M \tilde{d}}\left[1+\frac{m^2\Theta^2\tilde{d}^2}{12(1+q)}\right]. \tag{25}$$

Here it is assumed that $m^2\Theta^2\tilde{d}^2/[12(1+q)] \ll 1$. So the effect of rectification provides a self-shift δf of the resonance frequency and $\delta f/f_f \approx -2\delta I_0(\omega)/[3I_0(0)]$. A similar renormalization has been derived for the attenuation of SCW at resonance, so instead of the parameter of attenuation $1/\tilde{d}$ the value $\{1+5m^2\Theta^2\tilde{d}^2/[36(1+q)]\}/\tilde{d}$ must be used. The microscopic origin of these renormalizations is not obvious. However, for a rough qualitative interpretation it can be supposed that a reduction of the dc current flowing through the crystal results from the renormalization of the carrier drift length in a nonlinear system under simultaneous influence of the dc and ac voltage.

In spite of the general agreement between theory and experiment, there is some discrepancy, which is connected with variations of the magnitude of the effect as a function of the grating spacing Λ (or the grating constant K_g). In definite intervals of Λ, variations in deepness of the current minimum as a function of Λ agree qualitatively with Eq. (16), the deepness becomes larger with decreasing Λ. However, at relatively short (5–13 μm) grating periods (Fig. 7), the deepness of the minimum does not increase, it even decreases with decreasing grating spacing, which contradicts the theory. The same problem arises with the intensities of the signals of the second harmonic. This discrepancy between theory and experiment can be explained if we take into account additional contributions to the so-called quality factor of the resonance, which is the ratio between resonance frequency and damping factor of SCW. In the presented theory, the role of the quality factor is played by the parameter $\tilde{d}$ (or its renormalized value) which is associated with attenuation of SCW because of the limited carrier drift length. In Ref. 17, two additional factors were taken into account: the effect of trap saturation and diffusion of carriers. The effect of trap saturation means reduction of the maximal possible space-charge field of the grating with decreasing grating spacing because of shortage of the charge carriers provided by traps. In accordance with Ref. 17, but using the notations accepted in the present paper, the quality factor Q is determined by

$$Q^{-1} = \frac{E_0}{E_q} + \frac{1}{d} + \frac{E_D}{E_0}. \tag{26}$$

Here E_D is the so-called diffusion field, $E_q = eN/(\epsilon K_g)$ is the effective field characterizing the trap saturation effect, and N is the effective trap concentration. However, if we take into account the reduction of the internal field due to the parameter q and the remormalization of $\tilde{d}$ due to the rectification effect, the expression for Q^{-1} has a modified form

$$Q^{-1} = \frac{E_0}{E_q(1+q)} + \frac{1+5m^2\Theta^2\tilde{d}^2/[36(1+q)]}{\tilde{d}} + \frac{E_D(1+q)}{E_0}. \tag{27}$$

The fields E_D can easily be estimated,[17] and the estimate shows that the contribution of this factor can certainly be ignored for $\Lambda > 1$ μm. Then assuming that for $Bi_{12}GeO_{20}$ $\mu\tau = 1.6\times10^{-7}$ cm^2/V, $E_q = 50\times10^3$ V/cm (at $\Lambda = 10$ μm), $E_0 = 8\times10^3$ V/cm, $q = 0.7$, $m = 0.43$, and $\Theta = 0.628$, we can find that the maximum of Q occurs in the vicinity of $\Lambda = 5$–10 μm. The used fitting parameters E_q and $\mu\tau$ are consistent (within a factor of 1.5–2) with the published data.[17,24] So the experimental results are explained by the combination of attenuations caused by the trap saturation effect and the limited value of the drift length. Potentially, at higher values of m and Θ, an additional factor reducing Q arises, which is caused by the limitations imposed by strong nonlinear effects since the amplitude of SCW cannot be higher than the applied field [or the dc current $I_0(0)$ cannot be less than zero].

The experiments with overall rectification are rather informative from the point of view of material characterization. Formula (16) reveals a possibility to find many characteristics of the material by measuring the dc current as a function of modulation frequency. The parameters of interest can be found from the magnitude of the current at some specific values of the modulation frequency. They are $f = 0, f = f_f$ (where f_f is the position of the minimum), $f = f_C$ (where f_C is

the frequency of the intersection of the experimental curves obtained for different Θ), and $f=f_\infty \gg f_f$. For instance, the ratio $[I_0(f=f_\infty)-I_0(f=f_C)]/I_0(f=f_C)=m^2\Theta^2/[4(1+q)]$ allows us to find the parameter q from the corresponding experimental data. This is a unique opportunity since the magnitude of applied field inside the crystal, which is determined as $E_0/(1+q)$, can be found from relatively simple experiments. In principle, it is possible to use $I_0(f=0)$ or $I_0(\Theta=0)$ instead of $I_0(f=f_C)$. Selection of the preferable experimental parameters depends on the reliability of the available data. Calculations of q from the data for $\Theta=0.2\pi$ (Fig. 4) gives $q=0.7\pm0.1$ for $Bi_{12}GeO_{20}$ and $q=0.8\pm0.1$ for $Bi_{12}GeO_{20}$ (Fig. 7). Using the relationship

$$[I_0(f=f_\infty)-I_0(f=f_f)]/I_0(f=f_C)\approx m^2\Theta^2\tilde{d}^2/[8(1+q)],$$

which is correct for small m and Θ, one can find $\tilde{d}$, and then using relationship $f_f=1/(2\pi\tau_M\tilde{d})$, one can find τ_M. For instance, it follows from the experimental data for $Bi_{12}GeO_{20}$ at $\Lambda=50$ μm (where $f_f=430$ Hz and $f_C=740$ Hz) that $q=0.8$, $\tilde{d}=1.9$, $\tau_M=2\times10^{-4}$ s, and $\mu\tau=3.4\times10^{-7}$ cm^2/V. The data for $Bi_{12}GeO_{20}$ (Fig. 4, $\Theta=0.2\pi$) contain more uncertainty since $\Lambda=13.1$ μm corresponds to the situation where the quality factor includes remarkable contributions from other terms besides $\tilde{d}$. Note that a magnitude of $q=0.7$–0.8 means reduction of the applied field in the crystal approximately by 40–55 %, which agrees with our preliminary estimates (30–40 % in $Bi_{12}GeO_{20}$) obtained by measuring the electro-optic effect by scanning the crystal with a probe beam. Formula (16) demonstrates one more way of finding q. It can be done even without phase modulation, simply by comparing the current in the absence of the grating ($m=0$) and in the presence of the grating, since it follows from Eq. (16) that $[I_0(m=0)-I_0(m)]/I_0(m=0)=m^2/[2(1+q)]$ at $\Theta=0$. However, this technique needs very precise control of the illumination intensity to maintain the same photoconductivity when m is changed. Therefore, the technique used in our experiments is preferable.

The effect of second-harmonic generation of SCW is more difficult for experimental studies than the effect of rectification. The selected method of light diffraction from a phase grating formed by SCW is suitable only for photorefractive crystals. The data that can be obtained from these measurements are analogous to some of those obtained from experiments with rectification. For instance, the product $\tilde{d}\tau_M$ can be found from resonance peak positions, but $\tilde{d}$ potentially can be found from the ratios between the peak intensities in accordance with Eqs. (24) and (21). Note that a comparison of the peak positions in Figs. 9 and 10 with the theoretical predictions reveals a discrepancy between theory and experiment. It follows from Eqs. (22) and (24) that resonance frequencies have to correlate as 1:2:4, however, the experimental data in Fig. 10 correlate as 1:2.3:5.4 ($E_0=6$ kV/cm), as 1:2.5:5.6 ($E_0=8$ kV/cm), and as 1:2.5:5.9 ($E_0=10$ kV/cm). The qualitative explanation is based on the effect of a self-shift of the resonance frequency (25). Since the effect of a self-shift is more pronounced at the frequency of resonance excitation of the fundamental SCW (where the dc current is minimal due to rectification), the shift is higher for the higher frequency peak.

When the problems of second-harmonic generation are discussed, the question about the phase matching of the propagating waves arises. In nonlinear optics, pump waves, and generated waves are eigenmodes of the nonlinear medium where they propagate, so both modes have to satisfy a corresponding dispersion law. In our case, second-harmonic generation involves a combination of eigenmodes and forced waves, so the problem of phase matching vanishes since forced waves do not obey any dispersion law, and the desired wave vector and frequency of forced waves can be always selected.

Above we discussed nonlinear effects in the system of SCW that are similar to rectification and second-harmonic generation in nonlinear optics. However, the technique of excitation of SCW by an oscillating interference pattern used here provides one more nonlinear effect: scattering of SCW from static gratings of space charge resulting in spatial rectification and spatial doubling; effects that are not known in nonlinear optics. Spatial rectification and spatial doubling arise from the terms of the product $n(x,t)E(x,t)$ that includes simultaneously static and moving space-charge gratings. In the linear approach, static gratings are proportional to $m[\exp(iK_gx)+\text{c.c.}]$, whereas moving gratings (SCW) are proportional to $m\Theta\{\exp[i(K_gx-\Omega t)+\text{c.c.}]\}$. Then the product of the terms including static and moving gratings contains terms proportional to $m^2\Theta\exp(i\Omega t)$ and to $m^2\Theta\exp[i(K_gx-\Omega t)]$. The first term describes the appearance of an electric field in the crystal—homogeneous in space, but oscillating in time—i.e., spatial rectification; but the second term means generation of SCW with a doubled wave vector and the frequency Ω (spatial doubling). Spatial rectification has been studied in detail experimentally and theoretically.[23,25] A theoretical analysis of spatial doubling was given in Ref. 22, experimental data proving the validity of the model can be found in Ref. 25.

V. CONCLUSION

The effects of overall rectification and second-harmonic generation of SCW have been reliably detected. The effect of rectification results in an additional component of the dc current in the crystal due to interactions of SCW. The effect is strong, and this additional component reaches 20% of the initial current. A theory of the effect has been developed, which demonstrates excellent agreement with the experimental data. Two mechanisms of second-harmonic generation of SCW have been proposed, which are in a qualitative agreement with the experiments. A technique for the determination of the magnitude of the internal electric field in photoconductors has been proposed.

ACKNOWLEDGMENTS

M. P. Petrov and V. V. Bryksin thank the Russian Foundation for Basic Research (Grant No. 020217603) for financial support. F. Rahe acknowledges support of the Deutsche Forschungsgemeinschaft (Graduate college 695).

[1] R.F. Kazarinov, R.A. Suris, and B.I. Fuks, Semiconductors **6**, 500 (1972); *ibid.* **7**, 102 (1973).
[2] L. Solymar, D. J. Webb, and A. Gruennet-Jepsen, *The Physics and Application of Photorefractive Materials* (Clarendon Press, Oxford, 1996); Prog. Quantum Electron. **18**, 377 (1994).
[3] M.P. Petrov, V.V. Bryksin, V.M. Petrov, S. Wevering, and E. Krätzig, Phys. Rev. A **60**, 2413 (1999).
[4] P. Günter and J. -P. Huignard, *Topics in Applied Physics: Photorefractive Materials and Their Applications I and II*, edited by P. Günter and J.-P. Huignard (Springer-Verlag, Berlin, 1988), Vol. 61 and 62.
[5] B.I. Sturman, M. Aguilar, and F. Agullo-Lopez, Phys. Rev. B **54**, 13 737 (1996).
[6] L.-A. de Montmorillon, I. Biaggio, P. Delaye, J.-C. Launay, and G. Roosen, Opt. Commun. **129**, 293 (1996).
[7] P. Delaye, A. Blouin, D. Drolet, L.-A. Montmorillon, G. Roosen, and J.-P. Monchalin, J. Opt. Soc. Am. B **14**, 1723 (1997).
[8] S. Mansurova, N.K.S. Stepanov, and C. Dibon, Opt. Commun. **152**, 207 (1998).
[9] M. Ryzhii, V. Ryzhii, R. Suris, and C. Hamaguchi, Jpn. J. Appl. Phys., Part 2 **38**, L1388 (1999).
[10] I.K.M. Ryzhii, V. Ryzhii, R. Suris, and C. Hamaguchi, Jpn. J. Appl. Phys., Part 2 **38**, L6654 (1999).
[11] R.F. Zhdanova, M.S. Kagan, R.A. Suris, and B.I. Fuks, Sov. Phys. JETP **74**, 346 (1979).
[12] J.P. Huignard and A. Marrakchi, Opt. Commun. **38**, 249 (1981).
[13] S.I. Stepanov, V.V. Kulikov, and M.P. Petrov, Opt. Commun. **44**, 19 (1982).
[14] G. Hamel, D. Montchenault, B. Loiseaux, and J.-P. Huignard, Electron. Lett. **22**, 1031 (1986).
[15] H.C. Pederson, D.J. Webb, and P.M. Johansen, J. Opt. Soc. Am. B **15**, 2573 (1998).
[16] S. Mallick, B. Imbert, H. Ducollet, J.-P. Herriau, and J.-P. Huignard, J. Appl. Phys. **63**, 5660 (1988).
[17] B.I. Sturman, M. Mann, J. Otten, and K.H. Ringhofer, J. Opt. Soc. Am. B **10**, 1919 (1993).
[18] N. Blombergen, *Nonlinear Optics* (Benjamin, London, 1965).
[19] M. Bass, P.A. Franken, J.F. Ward, and G. Weinreich, Phys. Rev. Lett. **9**, 446 (1962).
[20] M.P. Petrov, V.V. Bryskin, S. Wevering, and E. Krätzig, Appl. Phys. B: Lasers Opt. **B73**, 669 (2001).
[21] N.V. Kukhtarev, V.B. Markov, S.G. Odoulov, M.S. Soskin, and V.L. Vinetskii, Ferroelectrics **22**, 949 (1979).
[22] V.V. Bryskin and M.P. Petrov, Phys. Solid State **40**, 1317 (1998).
[23] V.V. Bryskin and M.P. Petrov, Phys. Solid State **42**, 1808 (2000).
[24] V.M. Petrov, S. Wevering, M.P. Petrov, and E. Krätzig, Appl. Phys. B: Lasers Opt. **B68**, 73 (1999).
[25] M.P. Petrov, A.P. Paugurt, V.V. Bryksin, S. Wevering, and E. Krätzig, Phys. Rev. Lett. **84**, 5114 (2000).